JET PHENOMENOLOGY*

Michael H. Seymour

Rutherford Appleton Laboratory, Chilton,
Didcot, Oxfordshire. OX11 0QX. U.K.

Abstract

We discuss the phenomenology of jet physics at hadron colliders, concentrating on the internal structure of jets, which is studied using the jet shape distribution or subjet distributions.

*Contributed to Proceedings of Les Rencontres de la Valée d'Aoste: Results and Perspectives in Particle Physics, La Thuile, Italy, March 2–8, 1997.

1 Introduction

The inclusive jet rate in hadron collisions appears to be pretty well understood both experimentally [1–3] and theoretically [4–6]. The data are in good agreement with theory over seven orders of magnitude in rate, although with a hint of an excess at high E_T. There is little dependence on parton distribution functions and the overall theoretical error is estimated to be small.

However, one of the cross-checks often used to ensure that the jet data are well understood and modelled is the jet shape: a simple measure of the internal structure of the jets, specifically of how broad they are. Here the picture is not so clear [7–9]. The experiments are in good agreement with each other, giving us confidence in the data, but the experimental jets are considerably broader than predicted by hadron-level Monte Carlo event generators, and the dependence on the jet rapidity is not well modelled either. Next-to-leading order (NLO) calculations of the jet rate give a leading order (LO) prediction for the internal jet structure [10, 11]. Although these can be tuned to fit the data in any given bin in rapidity and transverse momentum, they do not give a good prediction of the dependence on those variables [12].

In this paper, we briefly summarize a recent study [13] of the extent to which these LO predictions should be affected by higher orders, resummation of logarithmically enhanced terms to all orders, and by including non-perturbative hadronization corrections. The conclusion is that all these effects are important, and we should not be surprised if LO does not agree well with data. As part of the study, we asked how well suited currently-used jet algorithms are for quantitatively probing the internal structure of jets. We found that the iterative cone algorithm [14], used by essentially all current experiments, is not infrared safe beyond the three-parton final state (i.e. beyond NLO for inclusive jet and dijet cross sections, but beyond LO for internal jet properties or three jet cross sections [15]). This makes them hopeless for quantitative studies. This problem can be solved by a slight modification to the algorithm [16], or better still by abandoning cone-type algorithms altogether in favour of the cluster-type $k_\perp$ algorithm [17, 18].

In Sect. 2, we describe the jet definitions in current use. Since each experiment defines their own slightly different variant of the cone algorithm, we concentrate on one in particular, DØ's [19], and only indicate the differences with respect to other experiments' where relevant. We then calculate, in a simple approximation, the cross section to next-to-next-to-leading order (NNLO) according to this algorithm, and explicitly show that it is not infrared safe. We discuss the solution proposed in [16].

In Sect. 3, we calculate the LO predictions for the jet shape in the various algorithms we have discussed. We estimate the effect of NLO corrections, power-suppressed hadronization corrections, and resummation of large logarithms to all orders.

In Sect. 4, we discuss another way of probing the internal structure of jets: by resolving subjets within them. This has many advantages over the jet shape, not least the fact that the subjet resolution variable gives us an extra handle to turn. We can choose to sit in a very perturbative regime, or to move smoothly into the hadronization regime, and eventually for very small resolution parameters, obtain the results of the usual jet shape as a limit of the subjet study.

Finally in Sect. 5, we make some concluding remarks.

2 Jet definitions and cross sections

All the algorithms we discuss define the momentum of a jet in terms of the momenta of its constituent particles in the same way, inspired by the Snowmass accord [20]. The transverse energy, E_T, pseudorapidity, η, and azimuth, ϕ, are given by:

$$\begin{aligned} E_{T\text{jet}} &= \sum_{i \in \text{jet}} E_{Ti}, \\ \eta_{\text{jet}} &= \sum_{i \in \text{jet}} E_{Ti}\, \eta_i / E_{T\text{jet}}, \\ \phi_{\text{jet}} &= \sum_{i \in \text{jet}} E_{Ti}\, \phi_i / E_{T\text{jet}}. \end{aligned} \tag{1}$$

We shall always use boost-invariant variables, so whenever we say 'angle', we mean the Lorentz-invariant opening angle $R_{ij} = \sqrt{(\eta_i - \eta_j)^2 + (\phi_i - \phi_j)^2}$. Also, whenever we say 'energy', we mean transverse energy, $E_T = E \sin\theta$.

2.1 The $k_\perp$ algorithm

We discuss the fully-inclusive $k_\perp$ algorithm including an R parameter [18]. It clusters particles (partons or calorimeter cells) according to the following iterative steps:

1. For every pair of particles, define a closeness

$$d_{ij} = \min(E_{Ti}, E_{Tj})^2 R_{ij}^2 \left(\approx \min(E_i, E_j)^2 \theta_{ij}^2 \approx k_\perp^2\right). \tag{2}$$

2. For every particle, define a closeness to the beam particles,

$$d_{ib} = E_{Ti}^2 R^2. \tag{3}$$

3. If $\min\{d_{ij}\} < \min\{d_{ib}\}$, *merge* particles i and j according to Eq. (1) (other merging schemes are also possible [17]).

4. If $\min\{d_{ib}\} < \min\{d_{ij}\}$, jet i is *complete.*

These steps are iterated until all jets are complete. In this case, all opening angles within each jet are $< R$ and all opening angles between jets are $> R$.

2.2 The DØ algorithm

Since this is the main algorithm we shall study, we define it in full detail. It is based on the iterative-cone concept, with cone radius R. Particles are clustered into jets according to the following steps:

1. The particles are passed through a calorimeter with cell size $\delta_0 \times \delta_0$ in $\eta \times \phi$ (in DØ, $\delta_0 = 0.1$). In the parton-level algorithm, we simulate this by clustering together all partons within an angle δ_0 of each other.

2. Every calorimeter cell (cluster) with energy above E_0, is considered as a 'seed cell' for the following step (in DØ, $E_0 = 1$ GeV).

3. A jet is defined by summing all cells within an angle R of the seed cell according to Eq. (1).

4. If the jet direction does not coincide with the seed cell, step 3 is reiterated, replacing the seed cell by the current jet direction, until a stable jet direction is achieved.

5. We now have a long list of jets, one for each seed cell. Many are duplicates: these are thrown away[1].

6. Some jets could be overlapping. Any jet that has more than 50% of its energy in common with a higher-energy jet is merged with that jet: all the cells in the lower-energy jet are considered part of the higher-energy jet, whose direction is again recalculated according to Eq. (1).

[1] In DØ, any with energy below 8 GeV are also thrown away. For jets above 16 GeV, this makes only a small numerical difference, which is not important to our discussion, so we keep them.

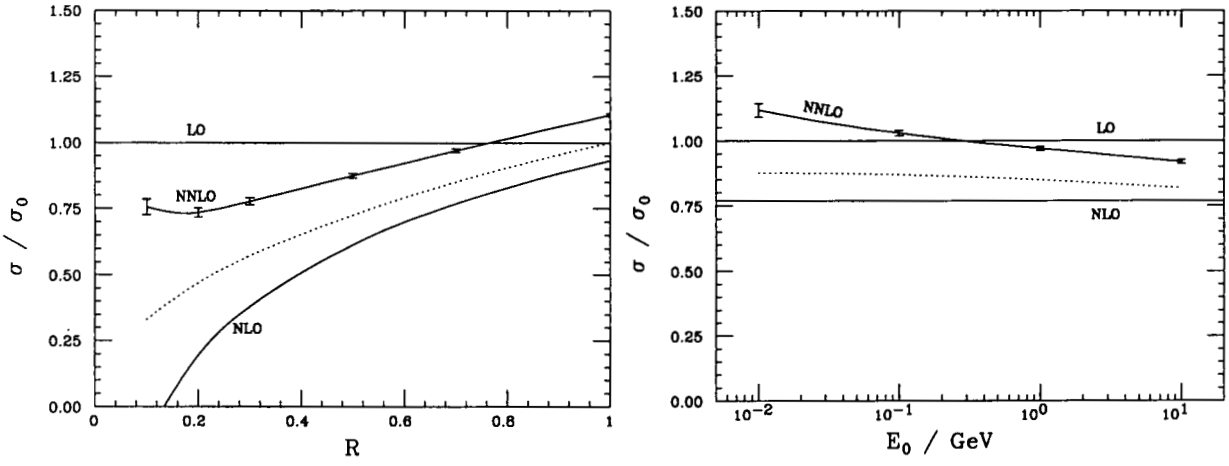

Figure 1: *The radius dependence with $E_0 = 1$ GeV (left) and seed cell threshold dependence with $R = 0.7$ (right) of the inclusive jet cross section in the DØ jet algorithm in fixed-order (solid) and all-orders (dotted) calculations. The error bars come from Monte Carlo statistics.*

7. Any jet that has less than 50% of its energy in common with a higher-energy jet is split from that jet: each cell is considered part only of the jet to which it is nearest.

Note that despite the use of a fixed cone of radius R, jets can contain energy at angles greater than R from their direction, because of step 6. This is not a particular problem. This is essentially also the algorithm used by ZEUS (PUCELL), except that their merging/splitting threshold is 75% instead of 50%. The CDF algorithm is similar again, and also uses 75%, but has a slightly different splitting procedure.

2.3 Jet cross sections

The issue of infrared safety in jet cross sections is discussed in [13]. There we define a class of jet definitions that we call 'almost unsafe', in which the definition appears at first sight to be unsafe, but that some minor detail makes it safe, although still unreliable. The iterative cone algorithm is of exactly this type, as can be seen in Fig. 1, where we show the cross section at successive orders, in the double-logarithmic approximation. The NNLO cross section depends logarithmically on the energy threshold of a calorimeter cell, and for an ideal calorimeter with zero threshold is clearly infinite. This divergence comes from the separation of events on the two-/three-jet boundary, and corresponds exactly to the divergence to negative infinity found for the three-jet cross section in [15].

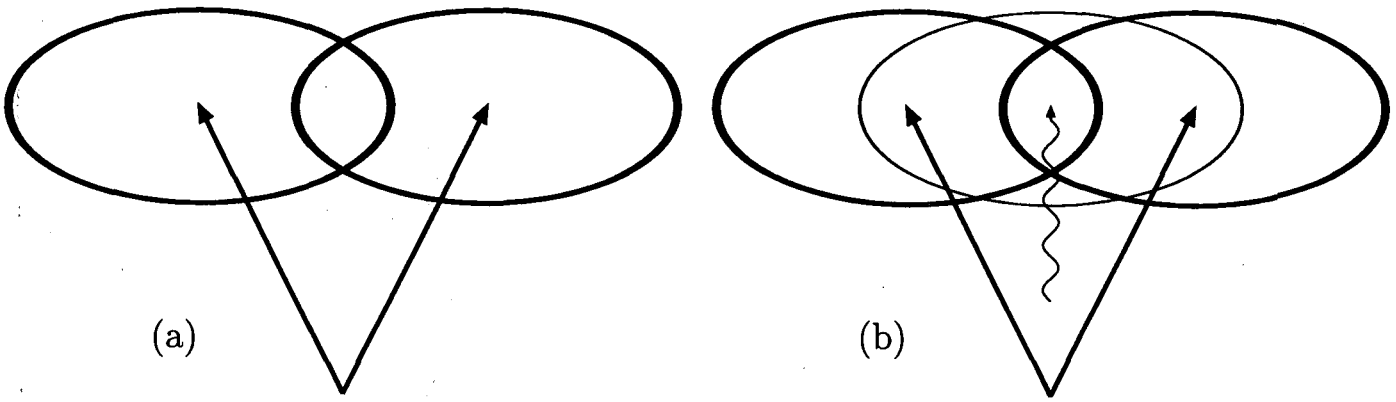

Figure 2: *Illustration of the problem region for the iterative cone algorithm. In (a), there are two hard partons, with overlapping cones. In (b) there is an additional soft parton in the overlap region.*

The strong E_0 dependence can be easily understood. It arises from configurations that have long been understood to be a problem in cone algorithms, where two partons lie somewhere between R and $2R$ apart in angle, but sufficiently balanced in energy that they are both within R of their common centre, defined by Eq. (1). This is illustrated in Fig. 2a. According to the iterative cone algorithm, each is a separate jet, because the cone around each seed cell contains no other active cells, so is immediately stable. Although the two cones overlap, there is no energy in the overlap region, so the splitting procedure is trivial, and it is classed as a two-jet configuration.

Now consider almost the same event, but with the addition of a soft parton, close to the energy threshold E_0, illustrated in Fig. 2b. If it is marginally below threshold, the classification is as above, with the soft parton being merged with whichever hard parton it is nearest. If on the other hand it is marginally above threshold, there is an additional seed cell. The cone around this seed encloses both the hard partons and thus a third stable solution is reached. Now the merging and splitting procedure produces completely different results. In either the CDF or DØ variants the result is the same: each of the outer jets overlaps with the central one, with the overlap region containing 100% of the outer one's energy. Thus each is merged with the central one, and it is classified as a one-jet configuration.

The classification is different depending on whether or not there is a parton in the overlap region with energy above E_0. Since the probability for this to occur can be estimated as $\sim \frac{2C_A}{\pi}\alpha_s \log E_T/E_0$, the inclusive jet cross section depends logarithmically on the energy threshold above which calorimeter cells are considered seed cells. Thus *the*

iterative cone jet definition is not fully infrared safe.

It is worth recalling how the $k_\perp$ algorithm completely avoids this issue, and remains infrared safe to all orders. Merging starts with the softest (lowest relative $k_\perp$) partons. Thus in the configuration of Fig. 2b, the soft parton is first merged with whichever hard parton it is nearer. Only then is any decision made about whether to merge the two jets, based solely on their opening angle. The algorithm has completely 'forgotten about' the soft parton, and treats the configurations of Figs. 2a and 2b identically. Thus, details of the calorimeter's energy threshold become irrelevant, provided it is significantly smaller than the jet's energy.

In Fig. 1, results were also shown from an all-orders calculation in the same approximation. As would be expected, the poor behaviour at small R has been tamed to give a well-behaved physical prediction. Surprisingly, the same is true of the E_0-dependence, which is much milder in the all-orders result than in the NNLO result.

This can be understood as a Sudakov-type effect. Although the fraction of events with a hard emission in the problem region is small, the probability of subsequent soft emission into the overlap of the cones in those events is large, $\sim \frac{2C_A}{\pi}\alpha_s \log E_T/E_0 \sim 1$. This is precisely the logarithmic behaviour seen in the NNLO result of Fig. 1. However, when going to the all-orders result, the probability of non-emission exponentiates, and we obtain

$$\frac{2C_A}{\pi}\alpha_s \log E_T/E_0 \longrightarrow 1 - \exp\left(-\frac{2C_A}{\pi}\alpha_s \log E_T/E_0\right) = 1 - \left(\frac{E_0}{E_T}\right)^{\frac{2C_A}{\pi}\alpha_s}, \qquad (4)$$

the much slower behaviour seen in the all-orders result of Fig. 1.

This result has a simple physical interpretation: in the 'all-orders environment', there are so many gluons around that there is almost always at least one seed cell in the overlap region and the two jets are merged to one. In our simple approximation, the coupling does not run. If we retained the running coupling, this statement would become even stronger, because the probability to emit soft gluons would be even more enhanced.

It is precisely this effect that has lead to the belief that the merging issue is a relatively unimportant numerical effect: *in the experimental environment it is.* However, expanding out the exponential of Eq. (4) as an order-by-order expansion in α_s, we obtain large coefficients at every order, and no hope of well-behaved theoretical predictions.

Thus, *if we are to study the internal properties of jets quantitatively, we must solve the overlap problem, to define jets in a perturbatively-calculable way.*

A simple solution to this problem was proposed some time ago [16]. It is a simple mod-

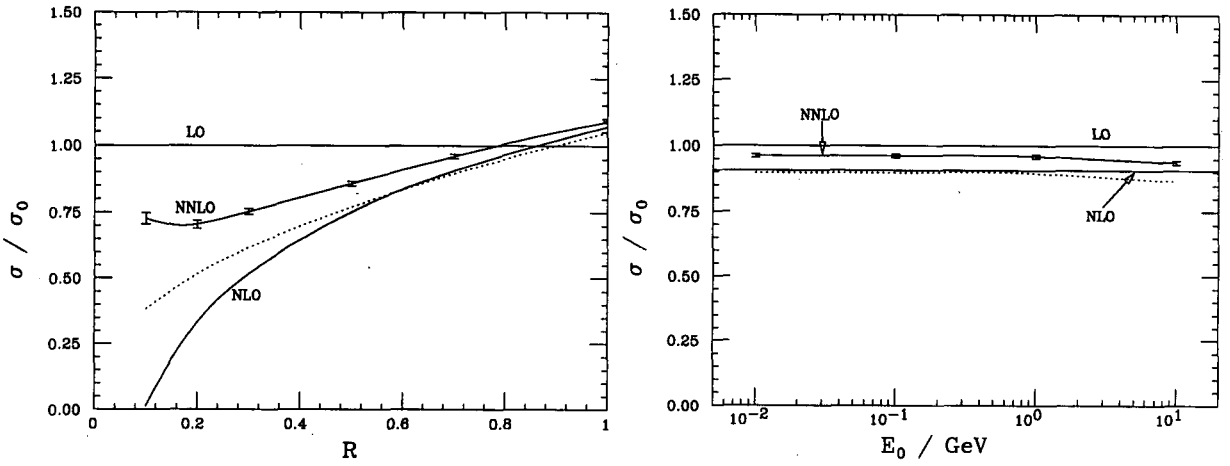

Figure 3: *The radius dependence with $E_0 = 1$ GeV (left) and seed cell threshold dependence with $R = 0.7$ (right) of the inclusive jet cross section in the improved iterative cone algorithm, in which midpoints of pairs of jets are used as additional seeds for the jet-finding, in fixed-order (solid) and all-orders (dotted) calculations.*

ification to the algorithm used in both the theoretical calculation and the experimental measurement:

> *After finding all possible jets using the seed cells, rerun the algorithm using the midpoint of all pairs of jets found in the first stage as additional seeds*[2].

This means that the results become insensitive to whether there was a seed cell in the overlap region, and hence to the energy threshold E_0. Cross sections are well-behaved and calculable order by order in perturbation theory, as shown in Fig. 3. Experimental results would be little changed by this modification (compare the all-orders results of Figs. 1 and 3), but the theoretical predictions would be enormously improved (compare the NNLO results of Figs. 1 and 3).

It should be stressed that this does not completely remove the problem of merging and splitting of overlapping cones. It merely relegates it to a procedural problem: one should state clearly the procedure one uses, and apply it equivalently to theory and experiment. Provided that that procedure uses information from all the jets in a democratic way (i.e. not keeping track of which jets came from seed cells, and which from the additional seeds), it will not spoil the improved properties of the algorithm.

We finish this section by noting that using the $k_\perp$ algorithm removes these problems

[2]To save computer time, it is sufficient to just do this for jet pairs that are between R and $2R$ apart.

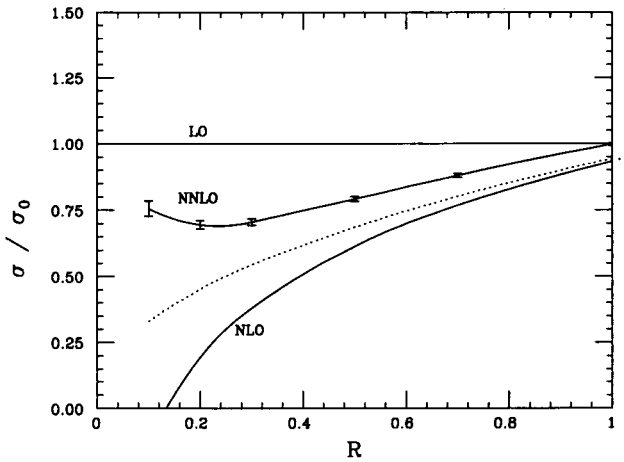

Figure 4: *The 'radius' dependence of the inclusive jet cross section in the $k_\perp$ jet algorithm in fixed-order (solid) and all-orders (dotted) calculations.*

completely. It is fully infrared safe, and has no overlap problem, because every final-state particle is assigned unambiguously to one and only one jet. We show results in Fig. 4. Unless there are factors of which we are unaware, abandoning the iterative cone algorithm and using the $k_\perp$ algorithm instead would be an even better solution than the previous one.

3 The jet shape

The jet shape is, at present, the most common way of resolving internal jet structure. It is inspired by the cone-type jet algorithm, but its use is not restricted to cone jets. It is defined by first running a jet algorithm to find a jet axis. The jet shape $\Psi(r;R)$ is then:

$$\Psi(r;R) = \frac{\sum_i E_{Ti}\,\Theta(r - R_{\mathrm{ijet}})}{\sum_i E_{Ti}\,\Theta(R - R_{\mathrm{ijet}})}, \tag{5}$$

where the sum over i can be over either all particles in the event, as used by CDF and DØ, or only those particles assigned to the jet, as used by ZEUS. We have found that using cone-type jet definitions, there is little difference between the two (less than 10% even at the jet edge). However, if the jet is defined in the $k_\perp$ algorithm, there are strong reasons for preferring the definition in which the sum is only over those particles assigned to the jet. For now, we concentrate on the more commonly-used definition in which the sum is over all particles. Thus Ψ is the fraction of all energy within a cone of size R around the

jet axis that is within a smaller cone of size r, also around the jet axis. Clearly we have $\Psi(R;R) = 1$, with $\Psi(r;R)$ rising monotonically in r.

It is often more convenient to work in terms of the differential jet shape:

$$\psi(r;R) = \frac{d\Psi(r;R)}{dr}. \tag{6}$$

Thus $\psi\, dr$ is the fraction of all energy within a cone of size R around the jet axis that is within an annulus of radius r and width dr, centred on the jet axis.

The NLO matrix elements for the jet cross section determine the jet shape at LO. However, we can avoid having to use the virtual matrix elements, by noting that they only contribute to $\psi(r;R)$ at exactly $r = 0$. Thus we can calculate $\psi(r;R)$ for all $r > 0$ from the tree level matrix elements and then get the contribution at $r = 0$ from the fact that it must integrate to 1, i.e.

$$\psi(r;R) = \delta(r) + \left(\psi_{\text{tree level}}(r;R)\right)_+, \tag{7}$$

where $f(r;R)_+$ is a distribution defined in terms of the function $f(r;R)$ by $f(r;R)_+ = f(r;R)$ for $r > 0$ and $\int_0^R f(r;R)_+ dr = 0$. It is straightforward to integrate the tree-level matrix elements to obtain the LO prediction for the jet shape. However, it is also useful to have an analytical approximation to the matrix elements to work with. This can be done using the modified leading logarithmic approximation (MLLA), in which we have contributions from soft and/or collinear final-state emission, and soft initial-state emission. For a quark jet we obtain [13]

$$\psi_q(r) = \frac{C_F\alpha_s}{2\pi}\left[\frac{2}{r}\left(2\log\tfrac{1}{Z} - \tfrac{3}{2}(1-Z)^2\right)\right]_+ + \psi_i(r), \tag{8}$$

where

$$Z = \begin{cases} \frac{r}{r+R} & \text{if } r < (R_{\text{sep}}-1)R, \\ \frac{r}{R_{\text{sep}}R} & \text{if } r > (R_{\text{sep}}-1)R \end{cases}, \tag{9}$$

and R_{sep} parametrizes the jet algorithm: $R_{\text{sep}} = 1$ in the iterative cone and $k_\perp$ algorithms, $R_{\text{sep}} = 2$ in the improved cone algorithm. For a gluon jet,

$$\begin{aligned} \psi_g(r) &= \frac{C_A\alpha_s}{2\pi}\left[\frac{2}{r}\left(2\log\tfrac{1}{Z} - (1-Z)^2\left(\tfrac{11}{6} - \tfrac{1}{3}Z + \tfrac{1}{2}Z^2\right)\right)\right]_+ \\ &+ \frac{T_R N_f\alpha_s}{2\pi}\left[\frac{2}{r}(1-Z)^2\left(\tfrac{2}{3} - \tfrac{2}{3}Z + Z^2\right)\right]_+ + \psi_i(r), \end{aligned} \tag{10}$$

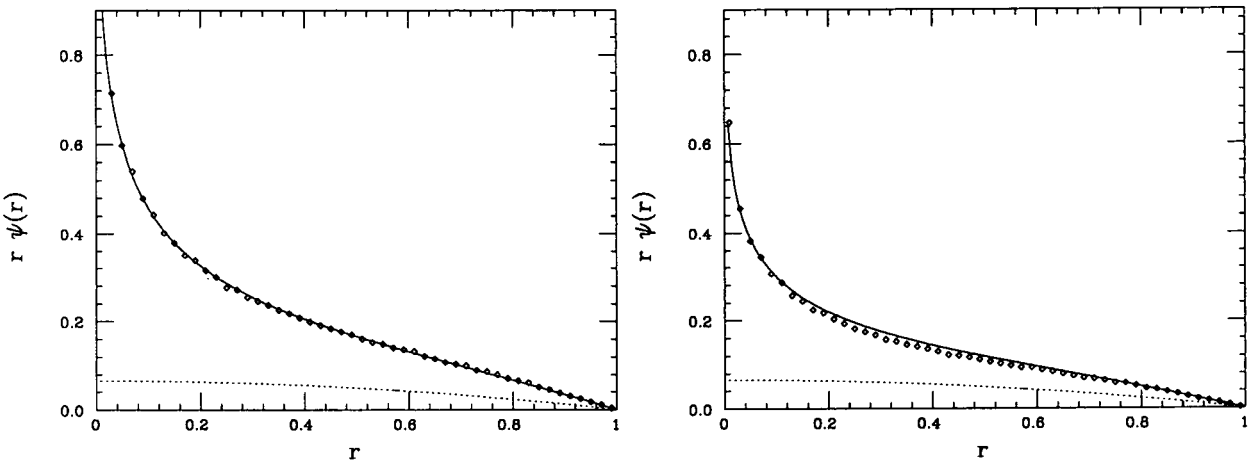

Figure 5: *The jet shape at leading order in the $k_\perp$ algorithm for a 50 GeV jet at $\eta = 0$ (left) and $\eta = 3$ (right), according to the exact tree-level matrix elements (points) and our analytical formulae (curves). The contributions of the initial-state component of the latter are shown separately as the dotted curves.*

where N_f is the number of flavours. The contribution $\psi_i(r)$ comes from initial-state radiation that is clustered into the jet, and is the same for quark and gluon jets. It is given by:

$$\psi_i(r) = \frac{C\alpha_s}{2\pi}\left[2r\left(\frac{1}{Z^2}-1\right)\right]_+, \tag{11}$$

where C is a factor that in principle depends on the kinematics and colour flow of the hard scattering, but in practice is well approximated by a constant, $C \sim C_F \sim C_A/2$, for which we use $C = C_A/2$ for all numerical results.

In Fig. 5 we show the results of both the full LO matrix element integration, and our analytical approximation to it, for the $k_\perp$ algorithm. As with all the numerical results in this paper, we use the CTEQ4M parton distribution functions [21]. We see remarkably good agreement between the full result and the analytical approximation. The contribution from initial-state radiation is shown separately, and is clearly essential for this good agreement.

Having seen that the analytical results approximate the full LO matrix element well, we move to higher orders to see how much we can improve them. We find that the jet shape in the iterative cone algorithm is strongly dependent on the seed cell threshold, as anticipated from the arguments of the previous section. We neglect it from further discussion.

In Fig. 6 we show results in the improved cone algorithm and the $k_\perp$ algorithm.

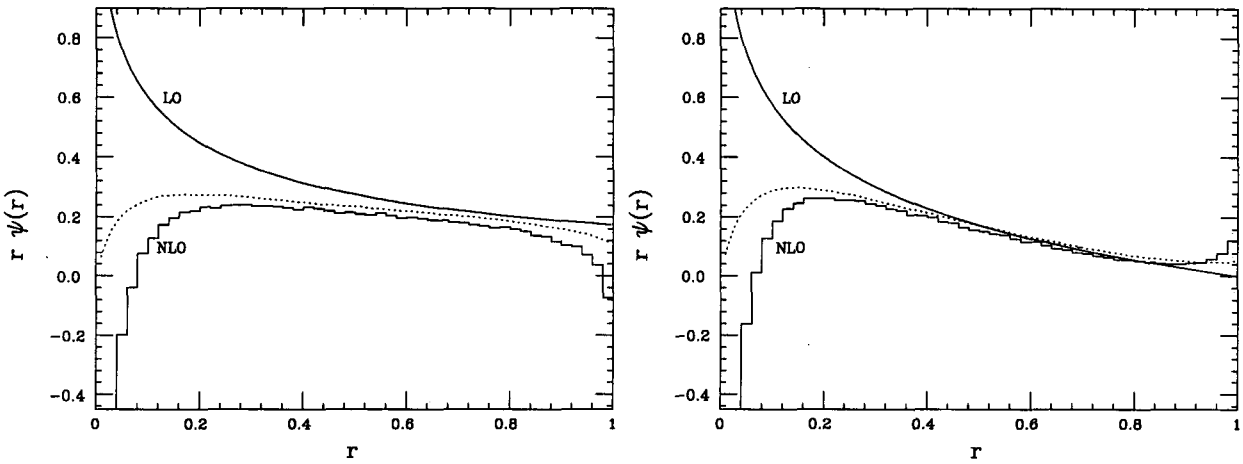

Figure 6: *The jet shape in the improved cone (left) and $k_\perp$ (right) jet algorithms in fixed-order (solid) and all-orders (dotted) calculations.*

In the improved cone algorithm, the NLO corrections are rather large (note that the normalization is outside the control of this approximation, and we should look at the shape of the corrections only). Close to the jet edge, they diverge to negative infinity, a typical 'Sudakov shoulder' effect [22], analogous to the C-parameter distribution in e^+e^- annihilation for $C \sim \frac{3}{4}$. The corresponding logarithms of $(R-r)$ must be resummed to all orders for a reliable prediction. The correction in both algorithms becomes large and negative at small r due to logarithmic terms in r, which can be resummed to all orders in α_s to give a physically-behaved prediction [13].

In the $k_\perp$ algorithm, the NLO corrections diverge to positive infinity near the edge of the jet. As discussed in [13], this is an artifact of the fact that we define the jet shape using all particles in the event. If we instead use only those particles assigned to the jet, we obtain a NLO result that is continuous at $r = R$. To avoid these large higher order terms, we recommend that in future the jet shape be defined using *only those particles assigned to the jet by the jet algorithm.*

A formalism has been developed over many years for summing various logarithmically-enhanced terms to all orders in α_s. In doing so, one inevitably ends up integrating over the Landau pole of the running coupling in perturbative calculations, signalling that non-perturbative confinement effects play a crucial rôle. In the Dokshitzer-Webber approach [23], these enter through *a priori* unknown, but universal, constants. The same one determines the jet shape as the average value of several event shapes in e^+e^- annihilation, like thrust. Thus jet shapes offer an excellent opportunity to test this universality, by comparing the quark-dominated jets of e^+e^- annihilation with the gluon-dominated jets

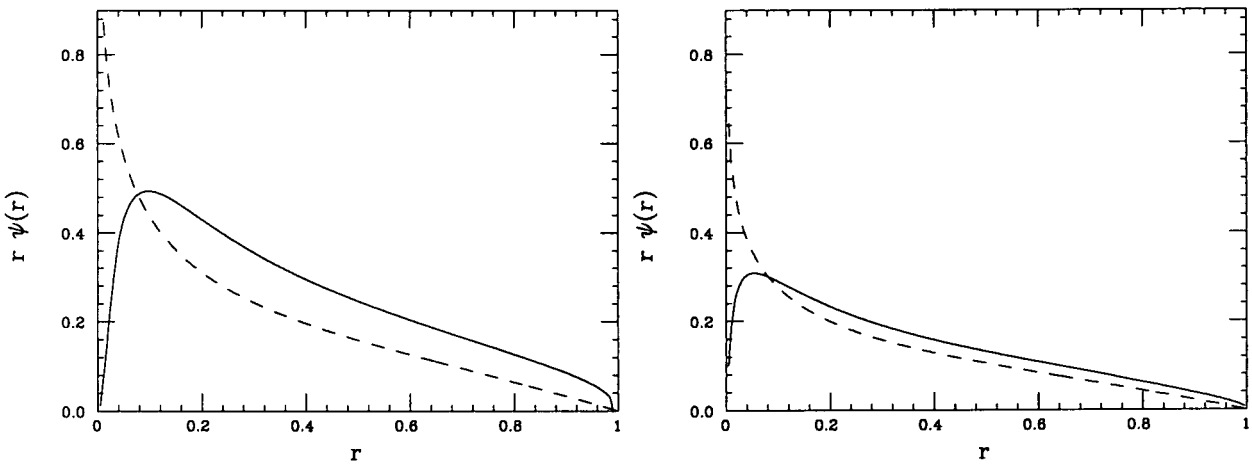

Figure 7: *Total effect of running coupling, power corrections and resummation on the shape of a 50 GeV (left) and 250 GeV (right) jet in the $k_\perp$ algorithm: LO (dashed) and with everything (solid).*

of hadron collisions. More details can be found in [13]. The net result of these corrections is shown in Fig. 7. At $E_T = 50$ GeV, they roughly double the amount of energy near the edge of the jet. Even at high transverse energy, $E_T = 250$ GeV, it is increased by about 50%, although most of this is accounted for by running coupling effects.

Looking at Figs. 6 and 7, one sees that neglected NLO, logarithmically enhanced, and power-suppressed terms are all very important in determining the jet shape distribution. We should not therefore be terribly surprised if LO predictions do not fit data very well. Quantitative studies of internal jet structure will only be possible once the long-awaited NLO corrections have been calculated.

4 Subjet structure of jets

The jet shape is largely inspired by cone-type jet algorithms, although it can be studied in cluster algorithms. In cluster algorithms however, it may seem more natural to study internal jet structure by using the same clustering algorithm, but stopping before the jet is complete, to define *subjets*. This is much more closely related to how we think that jets evolve: not by a gradual spreading in angle, but by iteratively splitting into subjets, subsubjets and so on, until eventually splitting to hadronic resonances and thence to stable hadrons.

Within the cluster algorithm, subjets can be defined by keeping track of which particles

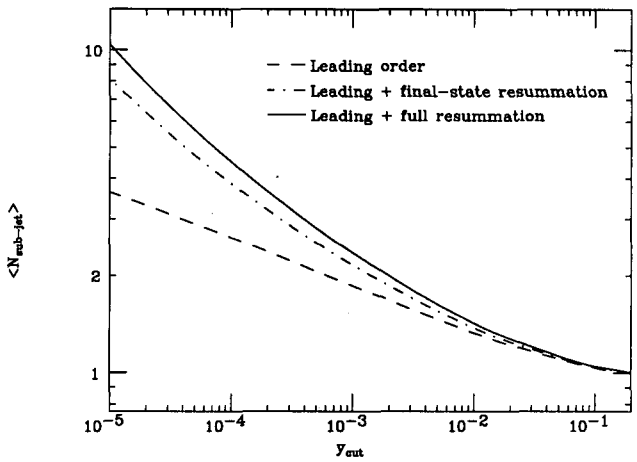

Figure 8: *Leading order (dashed) and resummed results for the subjet multiplicity in a 100 GeV jet at the Tevatron.*

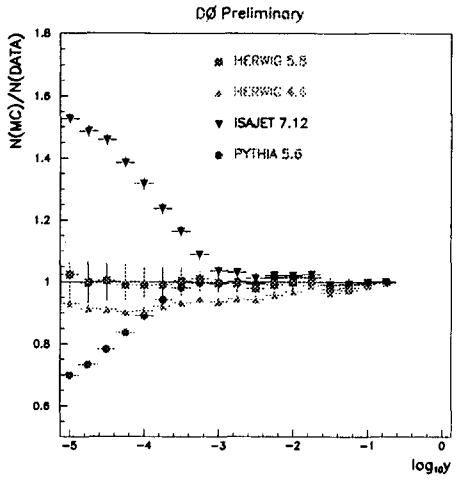

Figure 9: *The subjet multiplicity in a 300 GeV jet at detector level in various models, normalized to the data.*

ended up in the jet we are interested in, and rerunning the clustering algorithm using only those particles. The clustering is stopped when all the d_{ij} are above some cutoff:

$$y_{ij} \equiv \frac{d_{ij}}{E^2_{T\text{jet}}} > y_{\text{cut}}. \tag{12}$$

This is very similar to the way in which quark jets are studied in e^+e^- annihilation.

The simplest quantity one can imagine studying is the average number of subjets as a function of y_{cut}. As discussed in [24], when y_{cut} is small, the perturbative expansion is spoiled by large terms that arise at every order, $\alpha_s^n \log^{2n} y_{\text{cut}}$, and these must be summed to all orders for a reliable prediction. These come from final-state emission, and are identical to those in e^+e^- annihilation, as are part of the next-to-leading correction, $\alpha_s^n \log^{2n-1} y_{\text{cut}}$. However, at this level, initial-state radiation also contributes, making the results differ from the e^+e^- annihilation case. These terms can also be resummed, giving a prediction that is uniformly reliable for all y_{cut} [24]. The results are shown in Fig. 8. We see that the resummation is essential for small y_{cut}, and that the inclusion of the initial-state terms only makes a relatively small difference. In Fig. 9, we show the experimental results for a 300 GeV jet at detector level in comparison with various Monte Carlo event generators [25]. The agreement is remarkable, at least with models that include a full account of colour coherence [26]. At the left-hand side of the plot we are probing 300 GeV jets at a scale of only 1 GeV. More recent data can be found in [27, 28].

Once we have defined and counted the subjets, we can probe their distribution relative to the jet axis in just the same way as one normally does with the particles in a jet. The cutoff, $y_{\rm cut}$, can be tuned to choose to sit in a fully perturbative regime (large $y_{\rm cut}$), or a fully hadronized regime (for $y_{\rm cut} \to 0$ every hadron is considered a subjet of its own). That way we can start in a well-understood perturbative region, and gradually switch on hadronization in a controlled way. For example one can define the jet shape using subjets rather than particles, and one finds almost negligible parton→hadron corrections for reasonable $y_{\rm cut}$ values [27, 28].

5 Summary

In recent years there has been a growth of interest in the internal structure of jets. This is being given added impetus at the moment by the fact that a full NLO calculation is expected soon. By studying jets' internal structure, we are able to learn a great deal about the process by which hard partons are confined into jets of hadrons.

This renewed interest, and the ever-increasing accuracy of theoretical calculations, has prompted a critical evaluation of the quality of jet definitions in current use. We have found that they are insufficient for the level of accuracy required, and should be improved as described above, or better still replaced by cluster-type definitions like the $k_\perp$ algorithm.

Higher order corrections, all-orders resummation and non-perturbative hadronization corrections are all expected to be important in determining the jet shape, and we should not be surprised if LO calculations do not describe the data well.

Subjet studies offer a much greater degree of flexibility than the jet shape alone. One can choose to work in a highly-perturbative regime, which should be an ideal place to measure $\alpha_{\rm s}$ once we have NLO calculations, since most dependence on the absolute normalization and parton distribution functions drops out. Or one can choose to lower $y_{\rm cut}$ and study the onset of hadronization, eventually ending up at the usual hadronic final state. In this case, one has the confidence of knowing that the perturbative 'background' is under good control, and can ascribe deviations to the non-perturbative hadronization process.

It is to be hoped that with the NLO calculation to hand, and a greater degree of dialogue between theorists and experimenters, a new generation of internal jet measurements will emerge, shedding new light on the nature of jets and confinement.

References

[1] P. Melese, for the CDF Collaboration, 'Jet Physics at CDF', these proceedings; Fermilab–Conf–97/167–E.

[2] F. Abe *et al.*, CDF Collaboration, Phys. Rev. Lett. 77 (1996) 438.

[3] G.C. Blazey, for the DØ Collaboration, in Proceedings of the 31st Rencontres de Moriond: QCD and High-energy Hadronic Interactions, Les Arcs, France, 1996, p. 155.

[4] F. Aversa, P. Chiappetta, M. Greco and J.P. Guillet, Phys. Rev. Lett. 65 (1990) 401; Z. Phys. C46 (1990) 253;
F. Aversa, P. Chiappetta, L. Gonzales, M. Greco and J.P. Guillet, Z. Phys. C49 (1991) 459.

[5] S.D. Ellis, Z. Kunszt and D.E. Soper, Phys. Rev. Lett. 62 (1989) 726; Phys. Rev. D40 (1989) 2188; Phys. Rev. Lett. 64 (1990) 2121.

[6] W.T. Giele, E.W.N. Glover and D.A. Kosower, Nucl. Phys. B403 (1993) 633; Phys. Rev. Lett. 73 (1994) 2019.

[7] T. Heuring, for the DØ Collaboration, in Proceedings of the 10th Rencontres de Physique de la Vallée d'Aoste: Results and Perspectives in Particle Physics, La Thuile, Italy, 1996, p. 439.

[8] F. Abe *et al.*, CDF Collaboration, Phys. Rev. Lett. 70 (1993) 713.

[9] S. Abachi *et al.*, DØ Collaboration, Phys. Lett. B357 (1995) 500.

[10] S.D. Ellis, Z. Kunszt and D.E. Soper, Phys. Rev. Lett. 69 (1992) 3615.

[11] W.T. Giele, E.W.N. Glover and D.A. Kosower, 'Jet Investigations Using The Radial Moment', hep-ph/9706210.

[12] M. Klasen and G. Kramer, 'Jet Shapes in ep and $p\bar{p}$ Collisions in NLO QCD', hep-ph/9701247.

[13] M.H. Seymour, 'Jet Shapes in Hadron Collisions: Higher Orders, Resummation and Hadronization', hep-ph/9707338.

[14] F. Abe *et al.*, CDF Collaboration, Phys. Rev. D45 (1992) 1448.

[15] W.T. Giele and W.B. Kilgore, Phys. Rev. D55 (1997) 7183;
W.B. Kilgore, 'Next-to-leading Order Three Jet Production At Hadron Colliders', hep-ph/9705384.

[16] S.D. Ellis, private communication to the OPAL Collaboration;
D.E. Soper and H.-C. Yang, private communication to the OPAL Collaboration;
L.A. del Pozo, University of Cambridge PhD thesis, RALT–002, 1993;
R. Akers *et al.*, OPAL Collaboration, Z. Phys. C63 (1994) 197.

[17] S. Catani, Yu.L. Dokshitzer, M.H. Seymour, B.R. Webber, Nucl. Phys. B406 (1993) 187.

[18] S.D. Ellis and D.E. Soper, Phys. Rev. D48 (1993) 3160.

[19] B. Abbott, M. Bhattarcharjee, D. Elvira, F. Nang and H. Weerts, 'Fixed Cone Jet Definitions in DØ and $R_{\rm sep}$', Fermilab–Pub–97/242–E.

[20] J.E. Huth *et al.*, in *Research Directions for the Decade*, Proceedings of the Summer Study on High Energy Physics, Snowmass, Colorado, 1990, p. 134.

[21] H.L. Lai *et al.*, CTEQ Collaboration, Phys. Rev. D55 (1997) 1280.

[22] S. Catani and B.R. Webber, University of Cambridge preprint Cavendish–HEP–97/10, in preparation.

[23] Yu.L. Dokshitzer and B.R. Webber, Phys. Lett. B352 (1995) 451.

[24] M.H. Seymour, Nucl. Phys. B421 (1994) 545.

[25] R. Astur, in Proceedings of the 10th $\bar{p}p$ Workshop, Batavia, Illinois, 1995, p. 598.

[26] G. Marchesini, B.R. Webber, G. Abbiendi, I.G. Knowles, M.H. Seymour and L. Stanco, Computer Phys. Commun. 67 (1992) 465.

[27] R. Snihur, 'Subjet Structure of Jets at DØ', Fermilab–Conf–96/304-EE.

[28] D. Lincoln, 'QCD Results Using the $k_\perp$ Jet Finding Algorithm in $p\bar{p}$ Collisions at $\sqrt{s} = 1800$ GeV', Fermilab–Conf–97/149–E.